



This discussion paper is/has been under review for the journal Natural Hazards and Earth System Sciences (NHESS). Please refer to the corresponding final paper in NHESS if available.

Tsunami hazard potential for the equatorial southwestern Pacific atolls of Tokelau from scenario-based simulations

A. R. Orpin, G. J. Rickard, P. K. Gerring, and G. Lamarche

National Institute of Water and Atmospheric Research (NIWA), Private Bag 14-901, Kilbirnie, Wellington, New Zealand

Received: 14 January 2015 – Accepted: 28 June 2015 – Published: 30 July 2015

Correspondence to: A. R. Orpin (alan.orpin@niwa.co.nz)

Published by Copernicus Publications on behalf of the European Geosciences Union.

[Title Page](#)

[Abstract](#)

[Introduction](#)

[Conclusions](#)

[References](#)

[Tables](#)

[Figures](#)



[Back](#)

[Close](#)

[Full Screen / Esc](#)

[Printer-friendly Version](#)

[Interactive Discussion](#)



Abstract

5 Devastating tsunami over the last decade have significantly heightened awareness of the potential consequences and vulnerability to tsunami for low-lying Pacific islands and coastal regions. Our tsunami risk assessment for the atolls of the Tokelau Islands was based on a tsunami source–propagation–inundation model using Gerris Flow Solver, adapted from the companion study by Lamarche et al. (2015) for the islands of Wallis and Futuna. We assess whether there is potential for tsunami flooding on any of the village islets from a series of fourteen earthquake-source experiments that apply a combination of well-established fault parameters to represent plausible “high-risk scenarios” for each of the tsunamigenic sources. Earthquake source location and moment magnitude were related to tsunami wave heights and tsunami flood depths simulated for each of the three atolls of Tokelau. This approach was adopted to yield indicative and instructive results for a community advisory, rather than being fully deterministic.

15 Results from our modelling show that wave fields are channelled by the bathymetry of the Pacific basin in such a way that the swathes of the highest waves sweep immediately northeast of the Tokelau Islands. From our series of limited simulations a great earthquake from the Kuril Trench poses the most significant inundation threat to Tokelau, with maximum modelled-wave heights in excess of 1 m, which may last a few hours and include several wave trains. Other sources can impact specific sectors of the atolls, particularly from regional sources to the south, and northern and eastern distant sources that generate trans-Pacific tsunami. In many cases impacts are dependent on the wave orientation and direct exposure to the oncoming tsunami.

25 This study shows that dry areas remain around the villages in nearly all our “worst-case” tsunami simulations of the Tokelau Islands. Consistent with the oral history of little or no perceived tsunami threat, simulations from the recent Tohoku and Chile earthquake sources suggest only limited flooding. Where potential tsunami flooding was inferred from the modelling, recommended minimum evacuation heights above

Tokelau tsunami hazard potential

A. R. Orpin et al.

[Title Page](#)

[Abstract](#)

[Introduction](#)

[Conclusions](#)

[References](#)

[Tables](#)

[Figures](#)

[⏪](#)

[⏩](#)

[◀](#)

[▶](#)

[Back](#)

[Close](#)

[Full Screen / Esc](#)

[Printer-friendly Version](#)

[Interactive Discussion](#)



local sea level were compiled, with particular attention paid to variations in tsunami flood depth, subdivided into directional quadrants around each atoll. But complex wave behaviours around the atolls, islets, tidal channels and lagoons were also observed in our simulations. Wave amplitudes within the lagoons may exceed 50 cm, increasing any inundation and risks on the inner shoreline of the atolls, which may influence evacuation strategies. Our study shows that indicative, but instructive, simulation studies can be achieved even with only basic field information, due in part to the relative simplicity of the atoll topography and bathymetry.

1 Introduction

The potentially disastrous consequences of tsunami on low-lying islands and coastlines has only been reinforced in the aftermath of recent great earthquakes, namely Sumatra in 2004, Tonga-Samoa in 2009 and Tohoku (Japan) in 2011. Atolls have very low topographic relief, emerging only metres above sea-level (e.g. Woodroffe, 2008), such that even small rises in water level from storm set-up or tsunami could have the capacity to inundate lagoon-facing coastlines during spring tides (Ford et al., 2014). In this context inhabitants of atolls face challenges that differ from those of larger bedrock islands and mainland coasts, not least of which is the lack of topographic relief, and in turn, potential limitations to emergency evacuation procedures. In addition, the characteristic deep-ocean surrounds and steep approaches of atolls result in tsunami behaviour that differs from coastlines rimmed by shallow shelves (Sladen et al., 2007; Ford et al., 2014). Such rapid changes in depth on the approaches, a narrow reef crest and tidal platform, tidal channels, very thin or irregularly shaped islets, and a central lagoon that can be broad and deep, present computational challenges to the simulation of tsunami behaviour at resolutions meaningful for hazard assessments.

A suite of studies from the atoll islands of the Maldives documented the immediate impact of the tsunami generated from the Sumatran earthquake (e.g. Kench et al., 2006, 2008), along with sedimentological and morphological evidence from previous

Tokelau tsunami hazard potential

A. R. Orpin et al.

[Title Page](#)

[Abstract](#)

[Introduction](#)

[Conclusions](#)

[References](#)

[Tables](#)

[Figures](#)



[Back](#)

[Close](#)

[Full Screen / Esc](#)

[Printer-friendly Version](#)

[Interactive Discussion](#)



Tokelau tsunami hazard potential

A. R. Orpin et al.

[Title Page](#)

[Abstract](#)

[Introduction](#)

[Conclusions](#)

[References](#)

[Tables](#)

[Figures](#)

[⏪](#)

[⏩](#)

[◀](#)

[▶](#)

[Back](#)

[Close](#)

[Full Screen / Esc](#)

[Printer-friendly Version](#)

[Interactive Discussion](#)



events that extend back millennia (Klostermann et al., 2014). Throughout the Indian Ocean, the Sumatran earthquake also demonstrated a lack of community understanding of tsunami risks, appropriate response plans and the broader societal impacts (e.g. Kurita et al., 2007). The severity of the impact from such events has been a catalyst for international efforts to better understand and quantify tsunami risks. But many small-island nations are largely subsistence economies without the infrastructure to develop assessments of tsunami hazard.

Islands within the South Pacific are surrounded by distant seismogenic subduction margins with a history of great earthquakes capable of generating trans-Pacific tsunami (e.g. Hébert et al., 2001a, b). Regionally, the Southwest Pacific also has a history of intense tectonic activity, originating from the Pacific-Australia convergent plate boundary and the broad area of deformation in the North Fiji Basin-Lau Basin. There are numerous tectonically complex features associated with the Tonga and Vanuatu subduction zones (Pelletier et al., 1998) and recent studies have documented evidence of tsunami impacts resulting from regional sources (e.g. Lamarche et al., 2010). The atolls of Tokelau lie ~ 700 km north of the tip of the Tonga-Kermadec Trench (Fig. 1).

Tokelau is also one of five Pacific Island nations being supported under the New Zealand Government's Ministry for Civil Defence and Emergency Management (MCDEM) Pacific Tsunami Risk Management Project, which focuses on implementing key country disaster management priorities, early warning systems, public education and national exercises. To address that need NIWA undertook an initial assessment using a series of selected numerical simulations of tsunami inundation hazard for Tokelau, by exploring whether tsunami from distant or regional earthquake sources represent a significant risk. This approach was adopted to yield indicative and instructive results rather than being fully deterministic. The results were intended to help each Village Emergency Committee form their specific pre-determined response to tsunami warnings disseminated from the Pacific Tsunami Warning Centre in Hawaii via the Government of Tokelau, and to help ensure that emergency responses

to tsunami warnings are efficient and that any evacuations are not undertaken unnecessarily.

Our investigation closely follows a companion study by Lamarche et al. (2015, this issue), which examines tsunami risks in the remote French territory of Wallis and Futuna, Southwest Pacific, using Gerris Flow Solver to numerically model tsunami generation, propagation and inundation. We adapt Gerris to create a series of scenarios, which are not necessarily comprehensive, generated by earthquakes originating from the seismogenic Pacific Rim, the sources of which were identified and characterised using published data. Both studies build on the Gerris modelling work pioneered by Popinet (2012) that simulated the 11 March 2011 Japan (Tohoku) tsunami.

2 Study location

Tokelau is located just south of the equator, and consists of three relatively small atolls (nukus) that span approximately 160 km along a southeast–northwest axis, covering a total land area of approximately 12.25 km² within an EEZ of 290 000 km². The islands are located between 8°33′ S, 172°30′ W (Atafu) and 9°21′ S, 171°12′ W (Fakaofu), with Nukunonu approximately midway (Fig. 1). Tokelau is located ~ 480 km north of Samoa. All three atolls have a lagoon surrounded by a continuous matrix of fringing reef with the landmass, above the reef flat, made up of a series of islets. These are typically not more than a few hundred metres wide, and between 3 and 5 m above mean-sea level at their highest point. The tidal range in the Tokelau region is around 0.7 m. Tropical cyclones and ENSO-driven droughts are the two most common natural hazards affecting Tokelau at sub-decadal timescales. As far as we are aware there is no recorded or oral history of significant inundation damage on any of the atolls of Tokelau that can be attributed to distant or regional tsunamis.

Tokelau's population is currently just below 1500, split between the three atolls. On Atafu and Nukunonu there is a single village, whereas on Fakaofu the population is split

Tokelau tsunami hazard potential

A. R. Orpin et al.

[Title Page](#)

[Abstract](#)

[Introduction](#)

[Conclusions](#)

[References](#)

[Tables](#)

[Figures](#)

[⏪](#)

[⏩](#)

[⏴](#)

[⏵](#)

[Back](#)

[Close](#)

[Full Screen / Esc](#)

[Printer-friendly Version](#)

[Interactive Discussion](#)



between two islets (Fale and Fenua Fala). The villages are all located on the leeward (western or northwestern) sides of the atolls.

3 Assessing tsunami-flooding risks for Tokelau, scope and limitations

A number of studies have assessed deep water tsunami hazard around the Pacific Islands and Southwest Pacific, for example the first-generation tsunami scenario database developed for the Australian region by CSIRO as part of the Joint Australian Tsunami Warning Centre (JATWC) (Greenlade et al., 2009). However, deep-water tsunami models alone are not sufficient to develop an understanding of whether there is a potential tsunami inundation risk, particularly on atolls such as Tokelau where the seafloor rises very steeply from depths of between 2000 and 3000 m to the edge of the fringing reef at the sea surface.

In the current study modelling has been limited to distant and regional sources, where typically a warning would be provided by the Pacific Tsunami Warning Center. While tsunami caused by local submarine landslides or volcanism-related slope failure are other potential hazards, landslides big enough to cause any significant and widespread tsunami flooding will be rare and infrequent (e.g. Hébert et al., 2002; Goff, 2011). In addition, any consideration of slope instabilities in general will require near-complete coverage of high-resolution multibeam bathymetry of the slope surrounds. For Tokelau, and many other islands in the South Pacific, these data are not sufficiently dense, but as multibeam-bathymetry coverage continues to improve, local tsunami sources should also be examined. As such, local slope failures are not considered in the current study.

The tsunami inundation assessment was based on applying a tsunami source–propagation–inundation model to estimate whether there is potential for inundation of any of the village islets (motus) from a range of potential distant and regional tsunami sources. This assessment followed a four-step workflow:

Tokelau tsunami hazard potential

A. R. Orpin et al.

[Title Page](#)

[Abstract](#)

[Introduction](#)

[Conclusions](#)

[References](#)

[Tables](#)

[Figures](#)

[I◀](#)

[▶I](#)

[◀](#)

[▶](#)

[Back](#)

[Close](#)

[Full Screen / Esc](#)

[Printer-friendly Version](#)

[Interactive Discussion](#)



Tokelau tsunami hazard potential

A. R. Orpin et al.

[Title Page](#)[Abstract](#)[Introduction](#)[Conclusions](#)[References](#)[Tables](#)[Figures](#)[I◀](#)[▶I](#)[◀](#)[▶](#)[Back](#)[Close](#)[Full Screen / Esc](#)[Printer-friendly Version](#)[Interactive Discussion](#)

1. For each tsunamigenic-source area, simulate the maximum potential tsunami based on a series of the very large plausible earthquakes from published estimates of fault displacements and historical data (cf. Lamarche et al., 2015).
2. Establish a relationship between an earthquake warning (M_w and source location) and a potential tsunami risk (tsunami-wave height, H_{max} , and tsunami-flood depths, H_{in}).
3. Identify those source regions that pose a greater hazard and report these separately from other compiled sources.
4. Where potential tsunami flooding is identified, compile recommended evacuation heights above local sea level, with particular attention to variations in tsunami flood depth around the atolls.

4 Datasets and methods

4.1 Topographic and bathymetric data

The veracity of numerical simulations of tsunami are strongly dependant on the quality of seafloor topographic (bathymetric) data and the land topographic data for the area of inundation. The tsunami inundation modelling relied on an integrated representation of the nearshore bathymetry and topography drawn from available data sources. As noted in other modelling studies of island nations in the equatorial Pacific, whilst the paucity of high resolution data is a critical limitation, first-order quantification of tsunami behaviour and hazard assessments are still possible (e.g. Sladen et al., 2007). As such, maps of tsunami-inundation extent or tsunami-flood depth produced in the current study could not be produced accurately for each village islet. Inundation results should thus be seen as indicative only and more weight should be given to water levels.

Regional bathymetry from the General Bathymetric Chart of the Oceans datasets (GEBCO; www.gebco.net) were used to create the generalised bathymetry. Limited

Tokelau tsunami hazard potential

A. R. Orpin et al.

[Title Page](#)[Abstract](#)[Introduction](#)[Conclusions](#)[References](#)[Tables](#)[Figures](#)[I◀](#)[▶I](#)[◀](#)[▶](#)[Back](#)[Close](#)[Full Screen / Esc](#)[Printer-friendly Version](#)[Interactive Discussion](#)

high-resolution multibeam-bathymetric data from selected reef passages and approaches (< 300 m water depth) were acquired by the Royal New Zealand Navy Littoral Warfare Support Group in Tokelau for the Ministry of Foreign Affairs and Trade during Exercise Tropic Twilight in July 2011 (Jensen, 2011). These data were incorporated into a regional bathymetric grid along with soundings collected in 2005 and 2007 by the Navy from the upper- and mid-slope around all three atolls. We used remotely-sensed depth information from colour satellite images to complement these bathymetric data and to better parameterise the lagoons, reef flats and aprons. Hand-editing was required with iterative model runs to ensure sensible bathymetric profiles were achieved.

A significant limitation for Tokelau was the lack of high resolution topography over the emergent landmass and immediate tidal shallows. Elevation information for the atolls, islets and emergent reefs were generated from a range of data sources, all of which required careful filtering and hand editing. Vector data (generated from airborne radar) and feature catalogue information from the Multinational Geospatial Co-Production Programme (MGCP) and the New Zealand Defence Force (NZDF) are at a 30 m grid spacing and were incorporated where applicable. But given the very low elevation of the atolls, extensive and careful hand-editing of the elevation spot-heights was essential to ensure sensible elevations were incorporated into the topographic grid surface. Tree-tops were regularly listed as the land elevation and the spot-height density was often too low to create the grid resolution required to ensure useful model results. Other elevation information was gleaned from spot heights for features or infrastructure (e.g. tidal datum), rectified satellite images from the NZDF, and other published sources (e.g. Google Earth).

Due to the low data density around the villages, these elevation data were complemented by manual input of spot heights estimated from satellite images, following known natural bathymetric features such as beach-rock, reef flats or the beach face, along with man-made features such as sea-walls where elevations could be estimated from field photographs. To achieve a workable spot-height density the

Tokelau tsunami
hazard potential

A. R. Orpin et al.

[Title Page](#)[Abstract](#)[Introduction](#)[Conclusions](#)[References](#)[Tables](#)[Figures](#)[|◀](#)[▶|](#)[◀](#)[▶](#)[Back](#)[Close](#)[Full Screen / Esc](#)[Printer-friendly Version](#)[Interactive Discussion](#)

fringing-reef edge was assigned a height of 0 m, approximating a model mean sea-level datum (m.s.l.), both on the seaward and the lagoon sides of the atolls. This assumption appears compatible with the small number of available cross-sections of Tokelau village atolls from McLean (1993). An example of the final spot-height data density used in the simulations from the village of Atafu is shown in Fig. 2. To represent a “worst-case scenario”, a model sea-level datum was set at m.s.l. + 1 m to simulate a tsunami arriving at Mean High Water Spring tide (MHWS), visible as a MHWS strandline in aerial photographs that spatially approximates the base of the beach rise. The modelled topography for Atafu at m.s.l. and MHWS can be portrayed as a colour-ramp contour map (Fig. 3). Wave height and runup inundation depths cannot be extrapolated linearly from any given sea-level because of the complex behaviour of the wave interacting with the atoll as it shoals. A measure of the tsunami-wave runup over the emergent land (a proxy for inundation) is termed “ H_{in} ”. This differs from the maximum wave height, “ H_{max} ”, above a given sea-level. We anticipate that the two complete sets of simulations herein capture the range of realistic model outcomes and provide a broader understanding of the likely tsunami behaviour and risks for Tokelau. A schematic depiction of the sea-level elevations and inundation terminology used in the tsunami model simulations is shown in Fig. 4.

4.2 Earthquake-model scenarios to assess civil risks to Tokelau

For the purposes of exploring the civil risks of tsunami for Tokelau, the tsunami-generating earthquake sources can be classified into two basic scenarios based on event records: (1) regional sources that would have limited warning (a few hours) requiring a rapid response; and (2) distant sources that cause trans-Pacific events and would allow sufficient time for verification that a tsunami has occurred and appropriate warnings to be given. The earthquake scenarios selected in the current study are based on the largest Pacific earthquakes since 1900 and Pacific earthquakes of $M_w > 8.1$ since 1950 (Table 1). To be capable of generating a tsunami large enough to reach Tokelau and other Southwest Pacific Islands, ocean-wide or regional earthquakes

Tokelau tsunami hazard potential

A. R. Orpin et al.

[Title Page](#)[Abstract](#)[Introduction](#)[Conclusions](#)[References](#)[Tables](#)[Figures](#)[⏪](#)[⏩](#)[◀](#)[▶](#)[Back](#)[Close](#)[Full Screen / Esc](#)[Printer-friendly Version](#)[Interactive Discussion](#)

would typically have to be of magnitude greater than $M_w 8.0$. From this historical compilation a suite of modelling scenarios of the “most likely” sources of tsunami that may impact Tokelau was considered (Table 2). Paleo-tsunami research from the Pacific islands indicates that there is substantial geological evidence for destructive tsunami events with millennial-scale reoccurrence intervals (Goff et al., 2001a).

Tsunami propagation is controlled by seafloor topography and water depth along the path of the tsunami-wave train, while inundation is controlled by the coastal bathymetry, reef structures, topography above the shore line and human modification (e.g. Kunkel et al., 2006; Gelfenbaum, 2011; Popinet, 2012). Key physical parameters of the earthquake sources influence the amplitude of the tsunami wave at transoceanic distances, including focal depth, total slip and slip area, and azimuth (e.g. Hébert et al., 2001b). The final amplitude at a receiving shore is also strongly affected by focusing and defocusing effects, due to variations in bathymetry along the path of the tsunami (e.g. Hébert et al., 2001a).

4.3 Earthquake fault parameterisation

The current study considers only those tsunami generated by seafloor displacements associated with earthquake-fault ruptures. Tsunami excitation increases proportionally with the vertical displacement of the fault rupture on the seafloor, which in turn is related to the moment magnitude (M_w) of the generating earthquake (e.g. Okal, 1988) and the dip of the fault. Moment magnitude can be derived from an estimate of the fault-rupture’s physical parameters (length, width, depth and dip) using empirical relationships (e.g. Wells and Coppersmith, 1994). We use the Hanks and Kanamori (1979) empirical regression to estimate the fault-rupture parameters, where:

$$M_w = \frac{2}{3} \log(M_o) - 10.7 \quad (1)$$

where the seismic moment (M_o) is calculated from

$$M_o = \mu LWD \quad (2)$$

Tokelau tsunami hazard potential

A. R. Orpin et al.

[Title Page](#)[Abstract](#)[Introduction](#)[Conclusions](#)[References](#)[Tables](#)[Figures](#)[I◀](#)[▶I](#)[◀](#)[▶](#)[Back](#)[Close](#)[Full Screen / Esc](#)[Printer-friendly Version](#)[Interactive Discussion](#)

where μ is the rigidity modulus of the Earth's crust (3×10^{11} dyne cm^{-2}), and L and W are the fault length and width determined from bathymetry maps and literature review, respectively, and D the single event displacement provided in the literature. No uncertainties were assigned to these dimensions as we consider them to be maximum values. However, the relationship between earthquake magnitude and seafloor vertical displacement is complex, and in the absence of well-constrained field measurements may have multiple solutions and carry significant uncertainties (e.g. Okada, 1985). These uncertainties have not been formally quantified herein and are beyond the scope afforded by the current study.

Earthquake parameterisation herein (Table 2) is adapted from that described in more detail in the companion paper by Lamarche et al. (2015, this issue) from a scenario-based study of tsunami hazard for the South Pacific islands of Wallis and Futuna. Parameters were obtained from the literature and knowledge of regional tectonics and geodynamics (e.g. Johnson and Satake, 1993; Johnson et al., 1996; Lamarche et al., 2010, 2015; Goff et al., 2011b, 2012). Very large plausible earthquakes for each seismogenic region were estimated as a first order guide to assess potential tsunami behaviour, supported by observational data where possible. In some cases these earthquakes have no historic precedent per se, but represent high-risk or worst-case scenarios.

Earthquake fault parameters were compiled for the distant circum-Pacific deep subduction trenches of Japan, the Kuril Islands, Aleutian Islands, Cascadia, Peru and Chile, where earthquake magnitudes $> M_w$ 8.5 have been recorded (Table 1, Fig. 1). Data describing these historical earthquakes were readily available from the United States Geological Survey (earthquake.usgs.gov) and NOAA (www.ngdc.noaa.gov) databases. Of particular relevance to the current study are the source regions to the north and east of Tokelau, namely the Tokoku, Kuril and Aleutian Trench sources. The Tohoku fault parameters are based on the 11 March 2011 event, described in detail in Popinet (2012). The source model compiles 190 sub-faults previously defined by Okada (1985), and obtained by seismic inversion (Shao et al., 2011). Hence, the

Tokelau tsunami hazard potential

A. R. Orpin et al.

[Title Page](#)

[Abstract](#)

[Introduction](#)

[Conclusions](#)

[References](#)

[Tables](#)

[Figures](#)

[⏪](#)

[⏩](#)

[⏴](#)

[⏵](#)

[Back](#)

[Close](#)

[Full Screen / Esc](#)

[Printer-friendly Version](#)

[Interactive Discussion](#)



average slip noted in Table 2 is only a summary of this information. For Kuril, the fault parameters are based on two documented earthquakes (Rabinovich et al., 2008): (1) M_w 8.3 earthquake of 15 November 2006, the epicentre of which was located on the continental slope; and (2) M_w 8.1 earthquake of 13 January 2007 located in Kuril–Kamchatka Trench. Both these earthquakes caused trans-Pacific tsunamis that were recorded in Hawaii, the United States, Peru, Chile, and New Zealand. The 2007 event had a 400 km-long rupture, but a larger M_w 9 earthquake in 1952 from the same region suggests that longer ruptures are possible. Hence, a possible 1000 km-long rupture is speculated as a worst case scenario with a potentially high likelihood or re-occurrence (Table 2). According to the empirical relationship of Hanks and Kanamori (1979), such a rupture would result in a M_w 9.28 earthquake with ~ 17 m slip. Tsunamigenic-earthquake sources from the Aleutian–Alaska margin include events in 1957, 1964, and 1965 (Johnson et al., 1994). For the Aleutian Arc simulation, fault parameters are based on the earthquake of 9 March 1957, which Johnson et al. (1994) suggest had a rupture of 850 km in length and 10 m of slip, resulting in a M_w 8.6 event. Note that there are inherent complexities when modelling great earthquakes, and as highlighted by Greenslade et al. (2009), linear scaling becomes unreliable beyond M_w 9.2 and results in unrealistic earthquake rupture and slips lengths because peak slips occur only over a small area.

The regional sources were South Vanuatu Trench, central Vanuatu back-arc, North Vanuatu Trench, and the Tonga Trench. The Tonga Trench in particular experiences recurrent great earthquakes that have generated damaging tsunamis (e.g. Beavan, 2010; Lamarche et al., 2010; Okal, 2010). It therefore represents a significant and credible hazard to the surrounding South Pacific region. For the Tonga Trench specifically, four scenarios were developed: (1) rupture of the entire Tonga Trench, (2) rupture of the entire Tonga Trench with an arbitrary +1 m water height at the time of tsunami initiation to simulate potential climate-induced sea-level rise or storm-related set-up, (3) north Tonga Trench only; and, (4) central Tonga Trench only (as for the September 2009 earthquake). Lamarche et al. (2015, this issue) validated the assigned

fault parameters used in the scenarios against published post-tsunami observations made in Samoa and Futuna-Alofi.

4.4 Tsunami model parameterisation

The tsunami modelling was achieved using Gerris Flow Solver (Popinet, 2003). The Saint-Venant (or non-linear shallow water) equations (de Saint-Venant, 1871) used for numerical tsunami simulations have been integrated into Gerris, with details of the solution method and application using Gerris summarised in Popinet (2011) and Popinet (2012), respectively. In the time-dependent tsunami simulations, the adaptive grid generated in Gerris refines and coarsens to select the appropriate grid resolution to capture the tsunami wave evolution. This approach of dynamically adaptive mesh refinement can lead to orders of magnitude gains in computational efficiency compared to non-adaptive methods, of particular relevance in far-field trans-Pacific multi-kilometre scale simulations requiring simultaneous resolution of metre scale inundation processes. The initial wave elevation is generated from a source model derived using seismic data only. The study by Popinet (2012) of the 2011 Tohoku earthquake compared the tsunami simulated using Gerris with observational records from DART buoys, GLOSS tide gauges, and fine-scale flooding using satellite and field data; the results demonstrated that Gerris provided an accurate prediction of the long-distance wave and yielded considerable confidence that, in partnership with an accurate source model, Gerris can be applied to trans-Pacific tsunami simulations.

When running the model, there is a balance between accuracy (grid resolution) around the islands, and the need to complete the runs in a timely fashion (weeks rather than months of computation). For the scenarios used herein, the regional simulations have been run with spatial grid scales spanning 62 500 m down to a minimum of 31 m, while the distant simulations span grid scales of 208 498 m down to a minimum of 25 m. Here, the minimum grid size was limited by the resolution afforded by the elevation data for each of the atolls, which in most cases has significant uncertainty. A smaller grid size would yield meaningful results only if high-resolution data of sufficient density and

Tokelau tsunami hazard potential

A. R. Orpin et al.

[Title Page](#)

[Abstract](#)

[Introduction](#)

[Conclusions](#)

[References](#)

[Tables](#)

[Figures](#)

[⏪](#)

[⏩](#)

[◀](#)

[▶](#)

[Back](#)

[Close](#)

[Full Screen / Esc](#)

[Printer-friendly Version](#)

[Interactive Discussion](#)



accuracy existed, such as remotely-sensed laser-light elevations (LIDAR). As noted above, the current radar-derived vector data were not sufficient in this regard.

5 Results from tsunami model simulations

5.1 Distant-earthquake sources

5 The simulated maximum tsunami-wave heights above sea level (H_{\max}) were compiled for all distant sources, and the range of wave amplitudes is large (0.125–7.9 m) (Fig. 5). The largest earthquake sources can be seen from the elongated red streaks of high wave amplitudes around the Pacific basin. As the wave travels from the source region, it encounters topography in the form of sea floor bathymetry, seamounts, seamount chains, and other islands and larger land masses; each of which can accelerate, slow, and scatter the incident wave field, transforming the original single coherent wave, into a train of waves. The abrupt squared-off ends of some of the colour swathes mark the end of the model simulations: when the data indicated that the tsunami wave had long since passed through Tokelau, there was minimal risk of significant wave reflections, and there was no additional benefit in continuing the simulations.

15 The Kuril earthquake source generates particularly high wave amplitudes that mask other sources in this type of summary schematic. For this reason, Fig. 6 replicates Fig. 5, except that the large Kuril earthquake event has been excluded from the compilation of maximum tsunami sources. In comparing the upper frames in Figs. 5 and 6 it is noticeable that the Kuril event generates a response at the Tokelau Islands substantially larger than that of all the other simulations. The tsunami wave height in the vicinity of the Islands is around 50 cm excluding the Kuril event, but the wave height is potentially over 1 m with a Kuril event included. This is not simply a reflection of the relative initial earthquake magnitude of the Kuril event. Wave fields are channelled by the bathymetry of the Pacific basin in such a way that the largest wave heights miss the Tokelau Islands. Similarly, for the M_w 9.1 Cascadia event, the propagation

Tokelau tsunami hazard potential

A. R. Orpin et al.

[Title Page](#)

[Abstract](#)

[Introduction](#)

[Conclusions](#)

[References](#)

[Tables](#)

[Figures](#)

[I◀](#)

[▶I](#)

[◀](#)

[▶](#)

[Back](#)

[Close](#)

[Full Screen / Esc](#)

[Printer-friendly Version](#)

[Interactive Discussion](#)



Tokelau tsunami hazard potential

A. R. Orpin et al.

Title Page

Abstract

Introduction

Conclusions

References

Tables

Figures

⏪

⏩

◀

▶

Back

Close

Full Screen / Esc

Printer-friendly Version

Interactive Discussion



is such that no significant wave heights are registered at Tokelau. Importantly for hazard assessment, these simulations reinforce that earthquake event magnitude is not the only factor when determining the likelihood of significant waves at Tokelau. Here, the azimuth of the wave front and propagation direction across the seafloor are also significantly influential. The regional earthquake-source simulations show similar behaviour and interaction with the bathymetry.

Of the three atolls, the villages on Nukunonu and Fakaofu have more potential risk of inundation along their margins during the largest events because of their low and narrow land area. Our simulation suggests that the Tohoku event resulted in some modelled inundation, but much of the land surrounding the villages remained dry, notwithstanding the large uncertainties. Further validation of this modelled result could be yielded from observations after the Tohoku event in 2011 and Kuril earthquakes over recent decades, and incorporating these with information on the tidal state when the waves arrived. However, to the best of our knowledge there is no observational legacy of “unusual tides or surges” or other phenomena that could be linked to such events.

Modelled runup-height estimates for Tokelau were calculated using the maximum estimates from all distant-source simulations. These are portrayed as a colour ramp of the maximum tsunami-flood depth (in centimetres) above land, H_{in} , and a static impression of the summary maximum wave heights and inundation at Atafu can be obtained by integrating the full simulation time history into just a single image (Fig. 7). However, a particular challenge for our study was to ascertain enough topographic data to allow the model to adequately interpolate between the seaward and lagoon sides of each atoll. For the distant-earthquake simulations, Table 3 shows that the tsunami arrival times are in excess of 8 h for sources in the western part of the Pacific basin, and in excess of 13 h for Chile and Peru sources in the eastern part of the Pacific. Hence, warning times are relatively long.

Our simulations reinforced that each tsunami event is generally not characterized by the rapid passage of a simple, single wave front before returning to rest. Such events could persist for 2–3 h, during which time the wave field may remain at levels capable

of generating potential inundation (Table 3). The wave train may persist across the Pacific for days, but model simulations were stopped when the risk for further significant flooding was considered low.

5.2 Regional-earthquake sources

5 Seven regional scenarios were modelled, but only two (Northern Tip Tonga and Tonga Trench) resulted in wave heights over 10 cm at the Tokelau Islands and H_{\max} is typically less than 30 cm (Fig. 8). The regional sources used in this study are generally located to the south or south-west of the Tokelau Islands and, when combined with the fault orientation and bathymetry in this region, the simulations suggest that the Tokelau Islands are relatively “sheltered” (particularly by the Samoa Island chain) such that
10 wave heights exceeding 0.5 m are predicted to occur further west and east of the Tokelau Islands, but do not impact Tokelau.

Simulations of maximum tsunami inundation depth show some inundation on each of the islands resulting from the maximum-regional source simulations, but significant areas of land remain dry (Fig. 9). The amplitudes and patterns of inundation are comparable to the distant events excluding Kuril (Fig. 6), and reflect the influence of each island’s topography. Hence, the simulated land areas identified as dry for the
15 distant earthquake sources are also predicted to stay dry for regional sources.

The significant point of difference for the regional- versus the distant-earthquake source simulations is the arrival times of the first significant tsunami waves; a function of travel distance. Arrival times of 50 min (Northern Tip Tonga) to around 65 min (Tonga Trench) are to be expected, with event durations of 1–3 h (Table 3), so that lead times for implementing any emergency plan will be short for such regionally-generated events.
20

5.3 Summary of results from simulations

25 From the 14 potential distant and regional tsunami sources investigated in this hazard assessment, nearly all have land areas within the villages of the Tokelau Islands that

Tokelau tsunami hazard potential

A. R. Orpin et al.

[Title Page](#)

[Abstract](#)

[Introduction](#)

[Conclusions](#)

[References](#)

[Tables](#)

[Figures](#)

[I◀](#)

[▶I](#)

[◀](#)

[▶](#)

[Back](#)

[Close](#)

[Full Screen / Esc](#)

[Printer-friendly Version](#)

[Interactive Discussion](#)



Tokelau tsunami hazard potential

A. R. Orpin et al.

[Title Page](#)

[Abstract](#)

[Introduction](#)

[Conclusions](#)

[References](#)

[Tables](#)

[Figures](#)

[I◀](#)

[▶I](#)

[◀](#)

[▶](#)

[Back](#)

[Close](#)

[Full Screen / Esc](#)

[Printer-friendly Version](#)

[Interactive Discussion](#)



will remain dry. The scenarios sample a range of earthquake sources in terms of magnitude, orientation, and distance from the Tokelau Islands. Given that there have been eight tsunamigenic earthquakes $> M_w$ 8.1 since the year 2000, two of which were among the largest recorded earthquakes in the circum-Pacific since 1900 (Table 1), it is reasonable to assume that tsunami hazards are small to moderate. Collectively, the outcome that none of the modelled tsunami waves over-wash any of the atolls is broadly consistent with living memory of the islanders and oral history of little or no threat perceived of tsunami.

The static images used in this report represent a snap-shot of a tsunami-event scenario as the tsunami wave interacts with each of the atolls. However, other wave behaviour is evident when the complete wave passage is viewed as a movie, emphasising wave dynamics and refraction effects around the atolls, islets, tidal channels, and within the lagoons. Deep channels through the fringing-reef matrix in particular can allow for the propagation of far more tsunami energy than shoals protected by reef or islets (cf. Gelfenbaum et al., 2011). The simulations run at MHSW reinforce that during the largest events runup is also possible from the lagoon side of the atoll, as the reef flat does not provide a barrier to wave propagation.

6 Discussion

6.1 Comparison to other tsunami simulations for Pacific Ocean atolls

Central-Pacific islands are essentially surrounded by seismogenic subduction zones that are a defining geological feature of the Pacific Rim. But despite the large number of these tsunamigenic sources, previous simulation studies have suggested that the occurrence and behaviour of potentially dangerous trans-Pacific tsunami in the South Pacific is moderated by a combination of the fault-strike angle, arrival azimuth and deep-ocean bathymetry (e.g. Hébert et al., 2001a, b). Linear seafloor features, such as the large Hawaiian ridge and East Pacific Rise, can trap, scatter or redirect wave energy

Tokelau tsunami hazard potential

A. R. Orpin et al.

[Title Page](#)

[Abstract](#)

[Introduction](#)

[Conclusions](#)

[References](#)

[Tables](#)

[Figures](#)

[⏪](#)

[⏩](#)

[⏴](#)

[⏵](#)

[Back](#)

[Close](#)

[Full Screen / Esc](#)

[Printer-friendly Version](#)

[Interactive Discussion](#)



from tsunami sources. Results from our simulations agree with these prior studies and suggest that the deep surrounds of the Tokelau atolls reduces the tsunami wave height amplification in the region in general. The swathe of maximum wave heights from the Kuril simulation – the seismogenic source in our simulations that results in the strongest tsunami wave at Tokelau – passes immediately northeast of Tokelau, with amplification ~ 50 cm greater than that of waters around Tokelau (Fig. 5).

Peculiar to atolls as emergent features that can be impacted by tsunami, results from a previous study for the Tuamotu Archipelago of French Polynesia by Sladen et al. (2007) suggest that observational runup data from moderate tsunamis are consistent with offshore wave amplification, inferring that only moderate tsunami hazards might exist on reef-fringed atolls. They suggest that this behaviour is caused, in part, by the long wavelength relative to the short length of the steep bathymetric slope, and energy dissipation from wave reflection and breaking along the atoll crest. Our results are broadly consistent with these findings as none of the worst-case scenarios resulted in complete inundation of the Tokelau village islets, but simulated wave heights can exceed the tidal range nonetheless. As noted by Sladen et al. (2007), gaps in the reef may behave differently and present considerably higher risk with respect to elevated runup heights. Results from our simulations run at MHWS show elevated heights through tidal channels and within the lagoon (as discussed below). Given that atolls have such low relief there is little room for complacency, as evidenced by wave heights > 2 m from the 2004 Sumatra tsunami at the Maldives (Rabinovich and Thomson, 2007) and the accompanying destruction recorded on the Marshall Islands in the aftermath of the 2011 Tohoku tsunami (Ford et al., 2014).

With respect to impacts of tsunami in the wider equatorial Pacific from great earthquakes, following the M_w 9.0 Tohoku earthquake and tsunami in 2011, Ford et al. (2014) suggest that the impacts on Pacific Ocean atolls were relatively minor. Indeed, they report that since 1946, of the 26 tsunami events recorded at Kwajalein atoll in the Marshall Islands, the highest water level measured on a tidal gauge was only 0.38 m.

6.2 Behavioural characteristics of tsunami interactions within the atolls of Tokelau

The Gerris simulations generated significant wave amplitudes within the atolls themselves, which can be captured with the fine, adaptive local-grid resolution around each atoll. Snapshots using the Kuril-source experiment at MHWs demonstrate some of the behavioural characteristics of waves within the lagoons, taken using successive 100s increments from ~ 1 h after the arrival of the first wave-train at Atafu (Fig. 10). A range of solutions are obtained within the lagoons as the oceanic wave progresses from northwest to southeast through the Tokelau group. Here, the minimum spatial resolution of the simulation was adapted to 25 m relative to typical atoll scales of 5–10 km across, with resulting wave heights from 0.5 to 1.5 m. Given the grid resolution and other uncertainties (e.g. lagoon bathymetry), the general wave behaviours revealed in the simulations can be considered illustrative rather than quantifiable per se.

For Atafu a wave initially crossed the western reef (Fig. 10d), and then propagated eastward across the lagoon (Fig. 10e and f). There were also wave intrusions through the reef matrix on the northern and southern sides of the atoll, which interfered with the larger wave as it traversed the lagoon. Close inspection of these frames also reveals that the dry atoll regions (in black) changed in size as the waves both inundate and recede. For Nukunonu (Fig. 10g–i), a wave overtopped the northern reef, and then propagated southward across the lagoon, with another wave impinging from the north (Fig. 10i); these frames also show a series of waves generated by previous incursions into the lagoon propagating and interacting with each other. For Fakaofu (Fig. 10j–l) numerous waves interacted, produced by flow through Fakaofu's relatively complex fringing reef and islets, giving a more circular character to the wave fronts. Examination of the successive time increments (Fig. 10j–l) reveals a series of wave fronts that travel northwards and then to the northeast, eventually filling the entire lagoon.

NHESSD

3, 4391–4433, 2015

Tokelau tsunami hazard potential

A. R. Orpin et al.

[Title Page](#)

[Abstract](#)

[Introduction](#)

[Conclusions](#)

[References](#)

[Tables](#)

[Figures](#)

[⏪](#)

[⏩](#)

[⏴](#)

[⏵](#)

[Back](#)

[Close](#)

[Full Screen / Esc](#)

[Printer-friendly Version](#)

[Interactive Discussion](#)



Tokelau tsunami hazard potential

A. R. Orpin et al.

[Title Page](#)[Abstract](#)[Introduction](#)[Conclusions](#)[References](#)[Tables](#)[Figures](#)[I◀](#)[▶I](#)[◀](#)[▶](#)[Back](#)[Close](#)[Full Screen / Esc](#)[Printer-friendly Version](#)[Interactive Discussion](#)

Close inspection of the complex wave patterns within each atoll reveals changes in available dry land as the lagoon waves surge and recede. Together with wave amplitudes within the atolls that exceed 50 cm, there will likely be increased risks of inundation on sections of the lagoon shorelines. It is also apparent that the propagation timescale for the lagoon waves differs from that of the oceanic wave outside the atoll, raising potential for phase effects if the oceanic-wave setup interferes with the arrival of a wave from within the lagoon. As such, these complex wave fields and interactions may also influence evacuation strategies for villages and differs from coastal island settings, where retreat from the open ocean might be considered a safe option.

Here, Gerris solves the Saint-Venant equations (non-linear shallow water system), so will not reproduce the required dispersion relations as the topography shoals around the atolls. This dispersion is more correctly addressed using the so-called Boussinesq–Green–Naghdi variants of the shallow water systems (e.g. Panda et al., 2014, and references therein), and such equations can be solved using a new adaptive system called Basilisk (e.g., Popinet, 2014, 2015; Beatham et al., 2015).

6.3 Tsunami evacuation advisory: identifying key information relevant to end-users

In order to provide some kind of summary advisory for emergency planning for the Tokelau Islands in the event of a major tsunami, the combined maximum tsunami flooding results from the numerical modelling have been used to inform evacuation strategies. The results are presented in terms of the tsunami wave “runup height”: the maximum elevation on land to which the sea inundates above the initial sea level as a result of the tsunami event. Given the uncertainty of the topography used in this study, referencing the runup height back to sea-level was considered more meaningful and potentially provides a more tangible and less ambiguous point of reference for the islanders. For each island the highest runup from three cases is recorded. Two cases are based on the largest distant-sources: one with, and one without the Kuril simulation.

A third case records the highest runup simulated from the combined maximum regional sources.

Results from the current study and those from some other tsunami simulation studies for the south-central Pacific (e.g. Hébert et al., 2001a) emphasise the importance of wave orientation from specific tsunamigenic sources when considering inundation hazard for a particular location. To better recognise wave orientation as part of an advisory, for each of the semi-circular atolls, compass quadrants were used to provide a geographically practical means to assess the impact of the tsunami simulations on specific sections of the atoll and the main village(s) (Table 4). For each geographic region, the maximum runup height (in metres) is given above the specified local sea level: mean sea level (m.s.l.) and estimated Mean High Water Spring (MHWS).

In some cases, runup heights for simulations with sea-level at MHWS are lower than the equivalent earthquake sources run at m.s.l. This may seem counterintuitive and the reverse of what might be expected. An explanation for this behaviour may come from a simulation study by Gelfenbaum et al. (2011) that explored the effect of fringing reefs on tsunami inundation in American Samoa. Their study suggested that when fringing reefs are narrow (< 200 m wide), greater wave heights onshore are encouraged by shoaling interaction with the fringing reef. But as the reef width increases (\gg 200 m), dissipation of wave energy from bottom friction begins to dominate over shoaling and causes the tsunami wave heights to decrease. The fringing reefs around the atolls of Tokelau range in width from \sim 75–400+ m, but is variable laterally depending on the relative position of emergent islets. Whether the Tokelau reef flats are relatively wide when covered by the tide (MHWS), or exposed (m.s.l.) at the time of arrival spans the transition between shoaling or bottom-friction dominant wave behaviour.

For the geographic regions of each atoll, an area of dry land was considered “SAFE” if it was: (a) above the maximum inundation height, and (b) of “substantial” size. Given the relative uncertainties of the true atoll topography our advisory is therefore, conservative. Elevations considered to be the minimum “SAFE” evacuation height in the event of a major tsunami are compiled in Table 4. In some regions the result is

Tokelau tsunami hazard potential

A. R. Orpin et al.

Title Page

Abstract

Introduction

Conclusions

References

Tables

Figures



Back

Close

Full Screen / Esc

Printer-friendly Version

Interactive Discussion



flagged as “NOT SAFE”; these are regions that are particularly low lying, or where the estimated tsunami inundation is large. In such cases the advisory defaults to a precautionary approach, and to evacuate completely. As the villages of the Tokelau Islands are located on the western sectors of the atolls, hazards to infrastructure will also be sensitive to tsunami source and wave orientation.

The particular distant earthquake-source simulations responsible for the maximum tsunami runup are also identified in Table 4, and annotated accordingly as Chile (C), Kuril (K), Peru (P), and Tohoku (T). These tabulated results highlight that the largest magnitude earthquakes are not always responsible for the highest predicted runup around the atoll. The azimuth of the tsunami wave arrival is critical to the runup height. Furthermore, while trans-Pacific tsunami from Kuril might result in the maximum predicted inundation for the atoll in general, other earthquake sources may present greater risks for some quadrants of the atolls. But importantly, regardless of the earthquake source, the simulations predict that some areas of dry land would be preserved. The Tohoku tsunami is a recent event of significance that was very well observed around the Pacific (e.g. Popinet, 2012; Ford, 2013). All the simulations imply some quantifiable runup (i.e. something that could otherwise have been measured by a tide gauge, had one been installed) resulting from the Tohoku tsunami, but on a much smaller scale than that predicted for our Chile or Peru worst-case event, and significantly smaller compared to the Kuril event. The fact that there was no oral record of this tsunami by the Tokelauans might suggest that any increase in water height or behaviour was only minor and well within the tidal range of 0.7 m, consistent with the general findings of Ford et al. (2014) of relatively minor impacts in the Pacific Islands following the Tokoku tsunami.

In contrast, regional-earthquake sources generally result in lower tsunami runup compared to distant sources, but southern sectors of parts of the atolls are potentially less safe because regionally-sourced tsunami waves typically arrive from southern latitudes.

Tokelau tsunami hazard potential

A. R. Orpin et al.

Title Page

Abstract

Introduction

Conclusions

References

Tables

Figures



Back

Close

Full Screen / Esc

Printer-friendly Version

Interactive Discussion



Tokelau tsunami hazard potential

A. R. Orpin et al.

[Title Page](#)[Abstract](#)[Introduction](#)[Conclusions](#)[References](#)[Tables](#)[Figures](#)[Back](#)[Close](#)[Full Screen / Esc](#)[Printer-friendly Version](#)[Interactive Discussion](#)

For Atafu at MHWS, the trans-Pacific tsunami simulations predict a higher initial water level that covers most of the western geographical quadrant of the atoll and is deemed to be unsafe (Table 4). With the Kuril event specifically, there are still safe areas around the main village, and to the south and the east. But compared to the simulation with sea-level at m.s.l., the northern quadrant is not considered safe. Excluding a Kuril source, the predicted runups are lower, and all areas might be regarded as potentially safe zones for evacuation except the western quadrant. The results for Nukunonu show that Kuril- and Chile-earthquake sources dominate the maximum runups. Again for the simulation with sea level at m.s.l., safe evacuation heights for these sources can be found in each geographic quadrant of the atoll. In comparison to Atafu, for the simulation with the sea-level at MHWS, the relatively low terrain of Nukunonu enhances reef passages between the open ocean and the lagoon. The result is that many geographical regions of Nukunonu are typically not safe and the main village itself is potentially liable to be completely inundated from a Kuril or regionally sourced earthquake (Table 4). For the distant sources not including Kuril (but including the 2011 Tohoku event), the main village remains largely dry, consistent with observations. Like Nukunonu, Fakaofu is relatively low lying with many areas open to the ocean at the highest tides. For all simulations the southern and northwestern quadrants are typically not safe, as is the eastern quadrant for simulations at MHWS (Table 4). But importantly, for all simulations, including a Kuril source that predicted the maximum inundation, the main villages on Fakaofu are expected to retain safe dry areas.

Studies such as this can provide additional confidence to islanders and inform community evacuation strategies. In addition, the current study shows that provisional, but instructive, simulation studies can be achieved even with only basic field data, due in part to the relative simplicity of the atoll topography and the ability to glean elevation information from readily available data such as aerial photographs, selected beach profiles, and only partial multibeam coverage. In this case at least, the conical bathymetric form and low-relief characteristic of atolls is initially advantageous from a modelling perspective. But unquestionably, better bathymetric and topographic data

should encourage future studies and quantification of other hydrodynamic nuances peculiar to tsunami interactions with atolls.

7 Conclusions

A library of plausible, very large earthquake scenarios was simulated with the adaptive numerical model Gerris to explore the tsunami hazard for the three atolls of the Tokelau Islands. Areas of dry land remain around the villages in nearly all our tsunami simulations of the Tokelau Islands. A tsunami wave event may last a few hours and include several wave trains. Our limited series of simulations suggest that a great earthquake and trans-Pacific tsunami from the Kuril Trench poses the most significant inundation threat to the Tokelau Islands in general, but other sources can impact particular sectors of the atolls that are directly aligned to the oncoming tsunami. Consistent with other studies, our simulations show that tsunami wave orientation has an impact on inundation risk at specific locations around the atolls, particularly from regional sources to the south, and northern and eastern distant sources. The lagoon and deep passages through the fringing-reef matrix can also propagate significant tsunami wave energy, particularly if tides are high. Simulations suggest that complex wave fields and interactions may also occur within the lagoons, the heights of which could influence evacuation strategies for villages and differs from coastal island settings. The current study shows that provisional, but instructive, simulation studies can be achieved even with only basic field information, due in part to the relative simplicity of the atoll topography and bathymetry.

Acknowledgements. This tsunami hazard assessment was originally commissioned by the Government of Tokelau in collaboration with the New Zealand Government's Ministry for Civil Defence and Emergency Management (MCDEM). NIWA acknowledges their support for this study. The Geospatial Intelligence Organisation of the New Zealand Defence Force, and the New Zealand Hydrographic Authority of Land Information New Zealand kindly provided bathymetric and topographic data. The authors offer special thanks to Stéphane Popinet for

Tokelau tsunami hazard potential

A. R. Orpin et al.

[Title Page](#)

[Abstract](#)

[Introduction](#)

[Conclusions](#)

[References](#)

[Tables](#)

[Figures](#)



[Back](#)

[Close](#)

[Full Screen / Esc](#)

[Printer-friendly Version](#)

[Interactive Discussion](#)



his ongoing development of Gerris and insights into the modelling challenges. Thanks also to Emily Lane for her constructive internal review. This study was supported by the Marine Physical Resources Programme within NIWA's Coasts and Ocean Centre.

References

- 5 Beavan, J., Wang, X., Holden, C., Wilson, K., Power, W., Prasetya, G., Bevis, M., and Kautoke, R.: Near-simultaneous great earthquakes at Tongan megathrust and outer rise in September 2009, *Nature*, 466, 959–963, 2010.
- Beetham, E. P., Kench, P. S., Popinet, S., and O'Callaghan, J.: Simulating wave processes on coral reef platforms using a weakly dispersive Green–Naghdi solver, personal communication, 2015.
- 10 de Saint-Venant, A. B.: Théorie du mouvement non-permanent des eaux, avec application aux crues des rivières et à l'introduction des marées dans leur lit, *Comptes Rendus des séances de l'Académie des Sciences, Paris*, 73, 147–154, 1871.
- Ford, M., Becker, J. M., Merrifield, M. A., and Song, Y. T.: Marshall Islands fringing reef and atoll lagoon observations of the Tohoku tsunami, *Pure Appl. Geophys.*, 171, 3351–3363, doi:10.1007/s00024-013-0757-8, 2014.
- 15 Gelfenbaum, G., Apotsos, A., Stevens, A. W., and Jaffe, B.: Effects of fringing reefs on tsunami inundation: American Samoa, *Earth-Sci. Rev.*, 107, 12–22, doi:10.1016/j.earscirev.2010.12.005, 2011.
- 20 Goff, J.: Evidence of a previously unrecorded local tsunami, 13 April 2010, Cook Islands: implications for Pacific Island countries, *Nat. Hazards Earth Syst. Sci.*, 11, 1371–1379, doi:10.5194/nhess-11-1371-2011, 2011.
- Goff, J., Lamarche, G., Pelletier, B., Chague-Goff, C., and Strotz, L.: Predecessors to the 2009 South Pacific tsunami in the Wallis and Futuna archipelago, *Earth-Sci. Rev.*, 107, 91–106, 2011a.
- 25 Goff, J., Chagué-Goff, C., Dominey-Howes, D., McAdoo, B., Cronin, S., Bonté-Grapetin, M., Nichol, S., Horrocks, M., Cisternas, M., Lamarche, G., Pelletier, B., Jaffe, B., and Dudley, W.: Palaeotsunamis in the Pacific, *Earth-Sci. Rev.*, 107, 141–146, doi:10.1016/j.earscirev.2010.10.005, 2011b.

Tokelau tsunami hazard potential

A. R. Orpin et al.

[Title Page](#)

[Abstract](#)

[Introduction](#)

[Conclusions](#)

[References](#)

[Tables](#)

[Figures](#)

[⏪](#)

[⏩](#)

[⏴](#)

[⏵](#)

[Back](#)

[Close](#)

[Full Screen / Esc](#)

[Printer-friendly Version](#)

[Interactive Discussion](#)



Goff, J., Chagué-Goff, C., and Terry, J. P.: The value of a Pacific-wide tsunami database for risk reduction – putting theory into practice, *Geol. Soc. Spec. Publ.*, 361, 209–220, doi:10.1144/SP361.17, 2012.

Greenslade, D. J. M., Simanjuntak, M. A., and Allen, S. C. R.: An enhanced tsunami scenario database: T2, CAWCR technical report: 014, ISSN: Centre for Australian Weather and Climatic Research, Aust. Bureau Met. (CSIRO), Melbourne, Australia, 36 pp., ISSN 1836-019X, ISBN: 9781921605376 (pdf), 2009.

Hanks, T. C. and Kanamori, H.: A moment magnitude scale, *J. Geophys. Res.*, 84, 2348–2350, 1979.

Hébert, H., Heinrich, P., Schindelé, F., and Piatanesi, A.: Far-field simulation of tsunami propagation in the Pacific Ocean: impact on the Marquesas Islands (French Polynesia), *J. Geophys. Res.*, 106, 9161–9177, doi:10.1029/2000JC000552, 2001a.

Hébert, H., Schindelé, F., and Heinrich, P.: Tsunami risk assessment in the Marquesas Islands (French Polynesia) through numerical modeling of generic far-field events, *Nat. Hazards Earth Syst. Sci.*, 1, 233–242, doi:10.5194/nhess-1-233-2001, 2001b.

Hébert, H., Piatanesi, A., Heinrich, P., Schindelé, F., and Okal, E.: Numerical modeling of the 13 September 1999 landslide and tsunami on Fatu Hiva Island (French Polynesia), *Geophys. Res. Lett.*, 29, 1484, doi:10.1029/2001GL013774, 2002.

Jensen, P. D. (Lt.): Royal New Zealand Navy Littoral Warfare Support Group: Exercise Tropic Twilight – report of survey, surveyed by the Royal New Zealand Navy Deployable Hydrographic Survey Unit, Auckland, New Zealand, 96 pp., and digital data, 2009.

Johnson, J. M. and Satake, K.: Source parameters of the 1957 Aleutian Earthquake from tsunami waveforms, *Geophys. Res. Lett.*, 20, 1487–1490, 1993.

Johnson, J. M., Satake, K., Holdahl, S. R., and Sauber, J.: The 1964 Prince William Sound earthquake: joint inversion of tsunami and geodetic data, *J. Geophys. Res.-Sol. Ea.*, 101, 523–532, 1996.

Kunkel, C. M., Hallberg, R. W., and Oppenheimer, M.: Coral reefs reduce tsunami impact in model simulations, *Geophys. Res. Lett.*, 33, L23612, doi:10.1029/2006GL027892, 2006.

Lamarche, G., Pelletier, B., and Goff, J.: Impact of the 29 September 2009 South Pacific Tsunami on Wallis and Futuna, *Mar. Geol.*, 271, 297–302, doi:10.1016/j.margeo.2010.02.012, 2010.

Lamarche, G., Popinet, S., Pelletier, B., Mountjoy, J., Goff, J., Delaux, S., and Bind, J.: Scenario-based numerical modelling and the palaeo-historic record of tsunamis in Wallis

Tokelau tsunami hazard potential

A. R. Orpin et al.

[Title Page](#)[Abstract](#)[Introduction](#)[Conclusions](#)[References](#)[Tables](#)[Figures](#)[I◀](#)[▶I](#)[◀](#)[▶](#)[Back](#)[Close](#)[Full Screen / Esc](#)[Printer-friendly Version](#)[Interactive Discussion](#)

and Futuna, Southwest Pacific, Nat. Hazards Earth Syst. Sci. Discuss., 3, 2283–2346, doi:10.5194/nhessd-3-2283-2015, 2015.

McLean, R.: Existing and Proposed Extension to Gabion Seawall Protection in Tokelau: Environmental Impact Assessment, South Pacific Regional Environmental Programme (SPREP) Reports and Studies no. 62, SPREP, Apia, Western Samoa, 40 pp., ISBN 982-04-0047-3, 1993.

Okada, Y.: Surface deformation due to shear and tensile faults in a half-space, B. Seismol. Soc. Am., 4, 75, 1135–1154, 1985.

Okal, E. A.: Seismic parameters controlling far-field tsunami amplitudes: a review, Nat. Hazards, 1, 67–96, 1988.

Okal, E. A., Fritz, H. M., Synolakis, C. E., Borrero, J. C., Weiss, R., Lynett, P. J., Titov, V. V., Foteinis, S., Jaffe, B. E., Liu, P. L. F., and Chan, I. C.: Field survey of the Samoa tsunami of 29 September 2009, Seismol. Res. Lett., 81, 577–591, 2010.

Panda, N., Dawson, C., Zhang, Y., Kennedy, A. B., Westerink, J. J., and Donahue, A. S.: Discontinuous Galerkin methods for solving Boussinesq–Green–Naghdi equations in resolving non-linear and dispersive surface water waves, J. Comput. Phys., 273, 572–588, 2014.

Pelletier, B., Calmant, S., and Pillet, R.: Current tectonics of the Tonga–New Hebrides region, Earth Planet. Sc. Lett., 164, 263–276, 1998.

Popinet, S.: Quadtree-adaptive tsunami modelling, Ocean Dynam., 61, 1261–1285, 2011.

Popinet, S.: Adaptive modelling of long-distance wave propagation and fine-scale flooding during the Tohoku tsunami, Nat. Hazards Earth Syst. Sci., 12, 1213–1227, doi:10.5194/nhess-12-1213-2012, 2012.

Popinet, S.: Basilisk, available at: <http://basilisk.fr>, last established: 19 July 2015, 2014.

Popinet, S.: A quadtree-adaptive multigrid solver for the Serre–Green–Naghdi equations, J. Comput. Phys., submitted, 2015.

Popinet, S.: Gerris: a tree-based adaptive solver for the incompressible Euler equations in complex geometries, J. Comput. Phys., 190, 572–600, 2003.

Rabinovich, A. B. and Thomson, R. E.: The 26 December 2004 Sumatra tsunami: analysis of tide gauge data from the world ocean. Part 1. Indian Ocean and South Africa, Pure Appl. Geophys., 164, 261–308, doi:10.1007/s00024-006-0164-5, 2007.

Rabinovich, A. B., Lobkovsky, L. I., Fine, I. V., Thomson, R. E., Ivelskaya, T. N., and Kulikov, E. A.: Near-source observations and modeling of the Kuril Islands tsunamis of 15 November

2006 and 13 January 2007, Adv. Geosci., 14, 105–116, doi:10.5194/adgeo-14-105-2008, 2008.

Shao, G., Li, X., Ji, C., and Maeda, T.: Focal mechanism and slip history of the 2011 M_w 9.1 off the Pacific coast of Tohoku Earthquake, constrained with teleseismic body and surface waves, Earth Planets Space, 63, 559–564, 2011.

Sladen, A., Hébert, H., Schindel , F., and Reymond, D.: Evaluation of far-field tsunami hazard in French Polynesia based on historical data and numerical simulations, Nat. Hazards Earth Syst. Sci., 7, 195–206, doi:10.5194/nhess-7-195-2007, 2007.

Wells, D. L. and Coppersmith, K. J.: New empirical relationships among magnitude, rupture length, rupture width, rupture area, and surface displacement, B. Seismol. Soc. Am., 84, 974–1002, 1994.

Woodroffe, C. D.: Reef-island topography and the vulnerability of atolls to sea-level rise, Global Planet. Change, 62, 77–96, doi:10.1016/j.gloplacha.2007.11.001, 2008.

Tokelau tsunami hazard potential

A. R. Orpin et al.

[Title Page](#)

[Abstract](#)

[Introduction](#)

[Conclusions](#)

[References](#)

[Tables](#)

[Figures](#)

[|◀](#)

[▶|](#)

[◀](#)

[▶](#)

[Back](#)

[Close](#)

[Full Screen / Esc](#)

[Printer-friendly Version](#)

[Interactive Discussion](#)



Tokelau tsunami hazard potential

A. R. Orpin et al.

[Title Page](#)[Abstract](#)[Introduction](#)[Conclusions](#)[References](#)[Tables](#)[Figures](#)[I◀](#)[▶I](#)[◀](#)[▶](#)[Back](#)[Close](#)[Full Screen / Esc](#)[Printer-friendly Version](#)[Interactive Discussion](#)**Table 1.** Largest Pacific earthquakes and the approximate location of their epicentres since 1900 and Pacific earthquakes of $M_w > 8.1$ since 1950 (in order of decreasing magnitude). Data from USGS (see <http://earthquake.usgs.gov/earthquakes/world/historical.php>).

Date (dd mm yyyy)	Latitude (dec deg)	Longitude (dec deg)	M_w	Comment
22 May 1960	38.29° S	73.05° W	9.5	Chile
28 March 1964	61.02° N	147.65° W	9.2	Prince William Sound, Alaska
4 November 1952	52.76° N	160.06° E	9.0	Kamchatka, Russia
11 March 2011	38.322° N	142.369° E	9.0	Tohoku, near the east coast of Honshu, Japan
31 January 1906	1° N	81.5° W	8.8	Colombia–Ecuador
27 February 2010	35.846° S	72.719° W	8.8	Offshore Maule, Chile
4 February 1965	51.21° N	178.5° W	8.7	Rat Islands, Alaska
9 March 1957	51.56° N	175.39° W	8.6	Andreanof Islands, Alaska
3 February 1923	54° N	161° E	8.5	Kamchatka
13 October 1963	44.9° N	149.6° E	8.5	Kuril Islands
23 June 2001	16.264° S	73.641° W	8.4	Near the coast of south Peru
6 November 1958	44.329° N	148.623° E	8.3	Kuril Islands
19 August 1977	11.085° S	118.464° E	8.3	South of Sumbawa, Indonesia
4 October 1994	43.773° N	147.321° E	8.3	Kuril Islands
25 September 2003	41.815° N	143.91° E	8.3	Hokkaido, Japan region
15 November 2006	46.592° N	153.226° E	8.3	Kuril Islands
4 May 1959	53.351° N	159.645° E	8.2	Near the east coast of Kamchatka
16 May 1968	40.903° N	143.346° E	8.2	Off the east coast of Honshu, Japan
11 August 1969	43.478° N	147.815° E	8.2	Kuril Islands
17 February 1996	0.891° S	136.952° E	8.2	Irian Jaya region, Indonesia
4 March 1952	42.5° N	143° E	8.1	Hokkaido, Japan region
17 October 1966	10.807° S	78.684° W	8.1	Near the coast of central Peru
10 January 1971	3.132° S	139.697° E	8.1	Papua, Indonesia
3 October 1974	12.254° S	77.524° W	8.1	Near the coast of central Peru
22 June 1977	22.878° S	175.9° W	8.1	Tonga region
12 December 1979	1.598° N	79.358° W	8.1	Near the coast of Ecuador
13 January 2007	46.243° N	154.524° E	8.1	East of the Kuril Islands
1 April 2007	8.466° S	157.043° E	8.1	Solomon Islands
29 September 2009	15.489° S	172.095° W	8.1	Samoa Islands region

Tokelau tsunami
hazard potential

A. R. Orpin et al.

Table 2. Compilation of plausible “worst case” earthquake scenarios based on a combination of the largest historical earthquakes and/or established earthquake fault models (after Lamarche et al., 2015). The rake angle is 90° for all sources. Note the reduced size of the worst-case simulation for Chile reflects observational data and realistic fault geometries resulting from the M_w 9 May 1960 earthquake. (1) Date of earthquake used as reference; (2) magnitude used for the model, likely to differ from that of the reference earthquake; (3) fault length; (4) fault width; (5) length of slip along fault plane; (6) estimate after Popinet (2012) using a complex sub-fault model based on seismic inversion; and (7) estimate from composite USGS model, see http://earthquake.usgs.gov/earthquakes/eqinthenews/2009/us2009mdbi/finite_fault.php.

Name	Based on ¹	M_w^2	L^3 (km)	W^4 (km)	Slip ⁵ (m)	Dip ($^\circ$)	Strike ($^\circ$)
Regional sources							
North Vanuatu Trench	worst case	8.39	400	40	10	30	350
Vanuatu – back arc	worst case	7.96	200	30	6	40	170
South Vanuatu Trench	worst case	8.24	300	40	8	30	335
Tonga Trench	worst case	9.06	1000	80	20	30	195
Tonga 2009	29 September 2009	8.1	200 ⁷	50 ⁷	5–9.5 ⁷	57	342.5
Tonga Trench +1 m	worst case	9.06	1000	80	20	30	195
North Tonga Trench	worst case	8.16	300	40	6	60	100
Central Tonga Trench	worst case	8.57	600	50	10	30	200
Trans-Pacific distant sources							
Japan (Tohoku)	11 March 2011	9.0	700	50 ⁶	12.5	12	195
Chile	22 May 1960	9.29	920	120	32	12	10
Peru	13 August 1868	9.0	900	150	15	20	305
Aleutian Arc	9 March 1957	8.6	850	150	10	15	70
Cascadia	worst case	9.1	1050	70	17.5	15	350
Kuril Trench	worst case	9.28	1000	200	17	30	220

Title Page

Abstract

Introduction

Conclusions

References

Tables

Figures

I◀

▶I

◀

▶

Back

Close

Full Screen / Esc

Printer-friendly Version

Interactive Discussion



Tokelau tsunami hazard potential

A. R. Orpin et al.

Table 3. Arrival times in hours (h) and minutes (min) for waves from distant- and regional-earthquake simulations. The first occurrences of tsunami waves greater than 10 cm height are used to define initial arrival times to Tokelau and approximate tsunami event duration.

	Magnitude (M_w)	Atafu	Nukunonu	Fakaofu	Approximate duration
Distant sources					
Aleutian	8.6	8 h 15 min	8 h 25 min	8 h 30 min	~ 2 h
Chile	9.29	13 h 40 min	13 h 30 min	13 h 30 min	> 3 h
Kuril	9.28	8 h 20 min	8 h 25 min	8 h 35 min	> 3 h
Peru	9.0	15 h 15 min	15 h 10 min	15 h 00 min	> 2 h
Tohoku	9.0	8 h 55 min	8 h 55 min	8 h 55 min	> 3 h
Regional sources					
Northern Tip Tonga	8.16	50 min	50 min	50 min	> 70 min
Tonga Trench	9.06	70 min	65 min	60 min	> 3 h

[Title Page](#)[Abstract](#)[Introduction](#)[Conclusions](#)[References](#)[Tables](#)[Figures](#)[I◀](#)[▶I](#)[◀](#)[▶](#)[Back](#)[Close](#)[Full Screen / Esc](#)[Printer-friendly Version](#)[Interactive Discussion](#)

Table 4. Recommended minimum evacuation heights above local-sea level (m) for combined distant sources. To better recognise wave orientation as part of an advisory four geographic quadrants for each atolls are considered: north (N), south (S), east (E) and west (W). Due to the shape of Fakaofu the northeastern (NE) and northwestern (NW) quadrants of emergent land are noted. Labels refer to the distant sources of Chile (C), Kuril (K), Peru (P), and Tohoku (T), as the earthquake source region that yielded the maximum runup height from the series of tsunami simulations.

Atafu (sea-level at m.s.l.)	Main village (m)	N (m)	S (m)	E (m)	W (m)	
Source including Kuril	2.5 (K)	2.6 (K)	1.8 (K)	2.3 (K)	1.5 (K)	
Distant source excluding Kuril	2.0 (C)	1.1 (C)	1.5 (C)	2.3 (C)	1.3 (C)	
Regional sources	1.5	0.7	2.0	1.3	0.8	
Atafu (sea-level at MHWS)						
Source including Kuril	2.5 (K)	NOT SAFE	1.8 (K)	2.3 (K)	NOT SAFE	
Distant source excluding Kuril	1.6 (T)	1.2 (P)	1.5 (P)	1.2 (P)	NOT SAFE	
Regional sources	1.6	1.0	1.1	1.2	NOT SAFE	
Nukunonu (sea-level at m.s.l.)						
Distant source including Kuril	1.8 (K)	2.0 (K)	1.5 (C)	2.8 (C)	2.0 (K)	
Distant source excluding Kuril	1.8 (C)	1.2 (C)	1.5 (C)	2.8 (C)	1.0 (C)	
Regional sources	2.0	0.7	1.3	1.5	1.5	
Nukunonu (sea-level at MHWS)						
Distant source including Kuril	NOT SAFE	1.8 (K)	NOT SAFE	1.4 (C, K)	NOT SAFE	
Distant source excluding Kuril	1.4 (C, P)	1.1 (P)	NOT SAFE	1.4 (C)	1.0 (C)	
Regional sources	NOT SAFE	1.1	NOT SAFE	1.1	1.5	
Fakaofu (sea-level at m.s.l.)	Main village (m)	Fale (m)	NE (m)	S (m)	E (m)	NW (m)
Distant source including Kuril	2.9 (K)	1.7 (P)	2.3 (C)	NOT SAFE	1.6 (C)	NOT SAFE
Distant source excluding Kuril	2.2 (C)	1.7 (P)	2.3 (C)	NOT SAFE	1.6 (C)	NOT SAFE
Regional sources	1.5	1.3	0.8	1.8	1.1	NOT SAFE
Fakaofu (sea-level at MHWS)						
Distant source including Kuril	2.4 (P)	2.0 (P)	1.7 (P)	NOT SAFE	NOT SAFE	NOT SAFE
Distant source excluding Kuril	2.4 (P)	2.0 (P)	1.7 (P)	NOT SAFE	NOT SAFE	NOT SAFE
Regional sources	1.5	1.6	1.0	0.9	NOT SAFE	NOT SAFE

[Title Page](#)[Abstract](#)[Introduction](#)[Conclusions](#)[References](#)[Tables](#)[Figures](#)[I◀](#)[▶I](#)[◀](#)[▶](#)[Back](#)[Close](#)[Full Screen / Esc](#)[Printer-friendly Version](#)[Interactive Discussion](#)

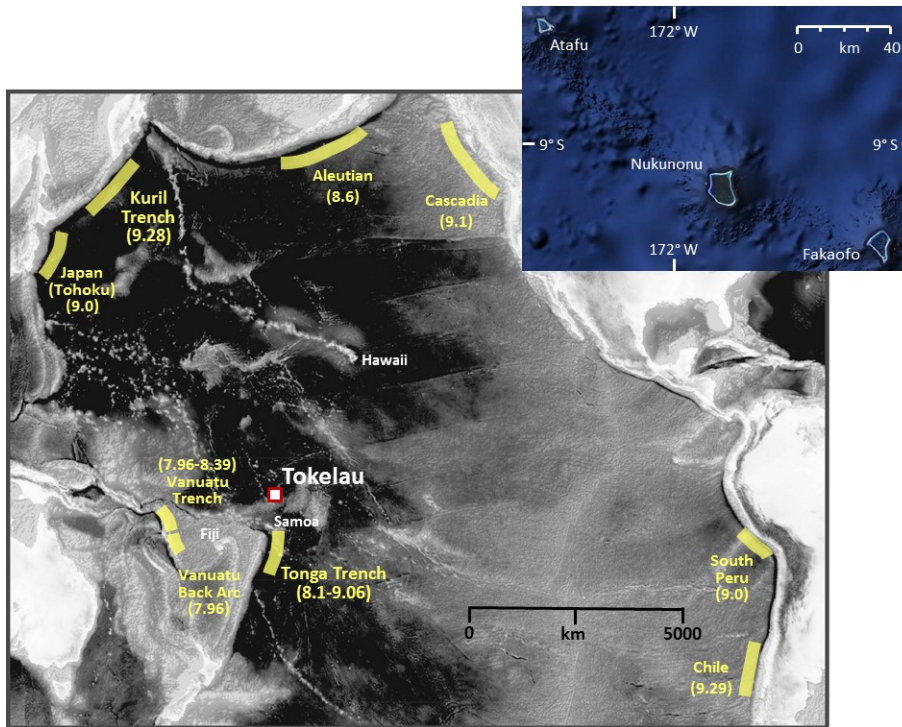


Figure 1. Location of the Tokelau Islands in the equatorial southwestern Pacific. The location of the atolls of Tokelau (Atafu, Nukunonu, and Fakaofu) are shown in the inset (base image from Google Earth). Known seismogenic sources are shown as light-yellow bars, and their earthquake magnitudes used in the scenario simulations used in this study are indicated (also summarised in Table 2 along with the fault-rupture geometries).

Tokelau tsunami hazard potential

A. R. Orpin et al.

[Title Page](#)

[Abstract](#)

[Introduction](#)

[Conclusions](#)

[References](#)

[Tables](#)

[Figures](#)

⏪

⏩

◀

▶

[Back](#)

[Close](#)

[Full Screen / Esc](#)

[Printer-friendly Version](#)

[Interactive Discussion](#)



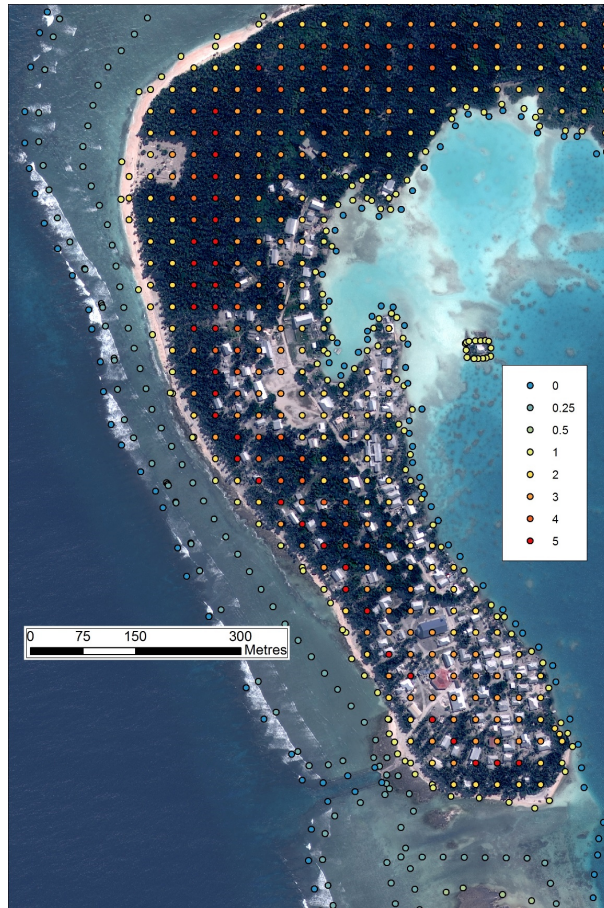


Figure 2. Example of derived spot-height data (in metres) with a grid spacing of ~ 30 m for a selected area around Atafu village. These new elevation (depth) data were used in the tsunami simulations.

[Title Page](#)

[Abstract](#)

[Introduction](#)

[Conclusions](#)

[References](#)

[Tables](#)

[Figures](#)

[⏪](#)

[⏩](#)

[◀](#)

[▶](#)

[Back](#)

[Close](#)

[Full Screen / Esc](#)

[Printer-friendly Version](#)

[Interactive Discussion](#)



Tokelau tsunami hazard potential

A. R. Orpin et al.

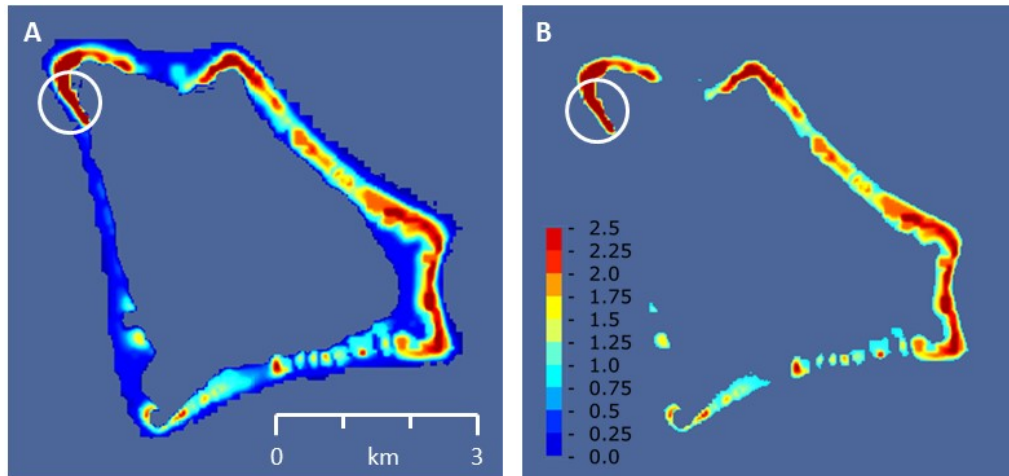


Figure 3. Example of the model-generated topography for Atafu, the smallest and northernmost atoll of the Tokelau group. The land topography is in metres above mean sea level (a.m.s.l.) **(a)**, and mean high water spring (MHWS) **(b)**, at a regular spatial resolution of 15 m. In the time dependent tsunami runs, the adaptive grid in Gerris will evolve and select the appropriate grid dimensions consistent with the tsunami wave as it approaches and subsequently passes the islands. The vertical land heights span a relatively limited range of 0.25–5 m. In contrast the surrounding ocean ranges from around zero at the reef edge to thousands of metres water depth within a short distance seaward of the shoreline. The lagoons have inferred depth ranges spanning many tens of metres (no verified measured depths were available). The village of Atafu is indicated by the circle in the northwestern corner of the atoll.

[Title Page](#)[Abstract](#)[Introduction](#)[Conclusions](#)[References](#)[Tables](#)[Figures](#)[⏪](#)[⏩](#)[◀](#)[▶](#)[Back](#)[Close](#)[Full Screen / Esc](#)[Printer-friendly Version](#)[Interactive Discussion](#)

Tokelau tsunami hazard potential

A. R. Orpin et al.

Title Page

Abstract

Introduction

Conclusions

References

Tables

Figures

◀

▶

◀

▶

Back

Close

Full Screen / Esc

Printer-friendly Version

Interactive Discussion

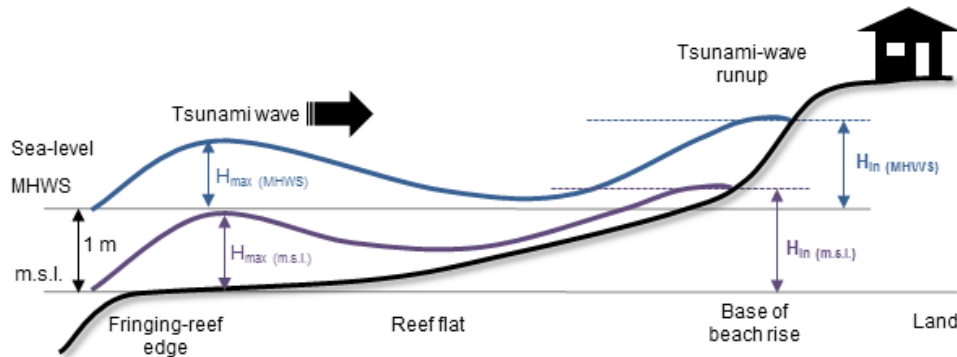


Figure 4. Schematic depiction of model sea-levels used in the tsunami simulations and terminology used to quantify tsunami-wave inundation. The horizontal and vertical dimensions are not to scale.

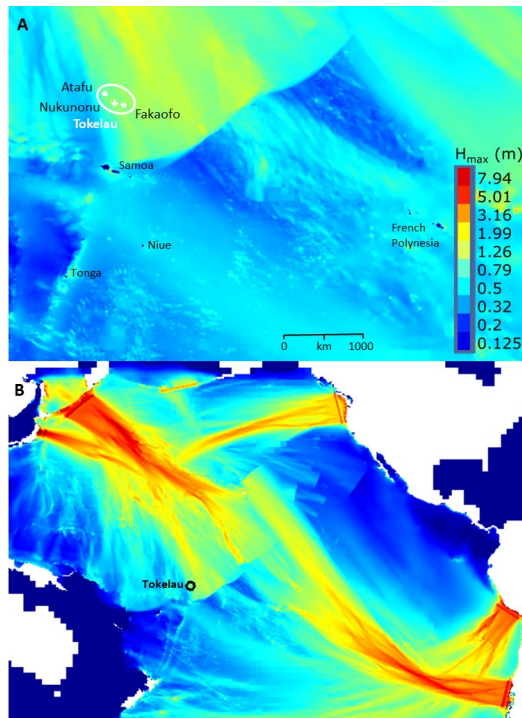


Figure 5. Summary of maximum wave heights for all distant sources. The top frame (a) provides a regional focus of the southwestern equatorial Pacific, with the Tokelau Islands outlined in white. The lower frame (b) provides a wider view of the Pacific Ocean and the distant, trans-Pacific tsunami source regions, with the Tokelau Islands outlined in black. Note that simulations stop after the majority of the tsunami-wave train has passed Tokelau, giving a truncated appearance to farthest extents of the wave fields. The height is plotted on a logarithmic scale (same for both images) to adequately capture the wide range of wave amplitudes in both frames (0.125 m in dark blue to over 7.9 m in red).

Tokelau tsunami hazard potential

A. R. Orpin et al.

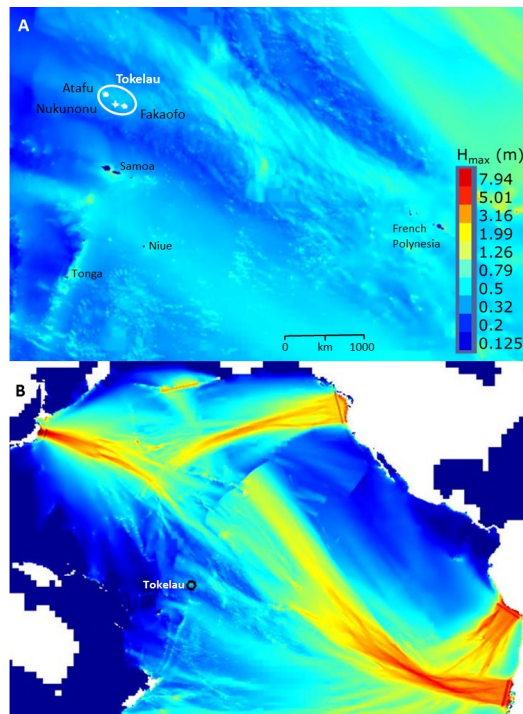


Figure 6. Summary of maximum wave heights for all distant sources excluding Kuril. The regional view (a), with the Tokelau Islands outlined in white, upper left. And a wider view of the Pacific Ocean (b), with the location of Tokelau indicated by the black circle. Note that simulations stop after the majority of the tsunami-wave train has passed Tokelau, giving a truncated appearance to farthest extents of the wave fields. The height is plotted on a logarithmic scale (same for both images) to adequately capture the wide range of wave amplitudes in both frames (0.125 m in dark blue to over 7.9 m in red).

Tokelau tsunami hazard potential

A. R. Orpin et al.

Title Page

Abstract

Introduction

Conclusions

References

Tables

Figures

◀

▶

◀

▶

Back

Close

Full Screen / Esc

Printer-friendly Version

Interactive Discussion

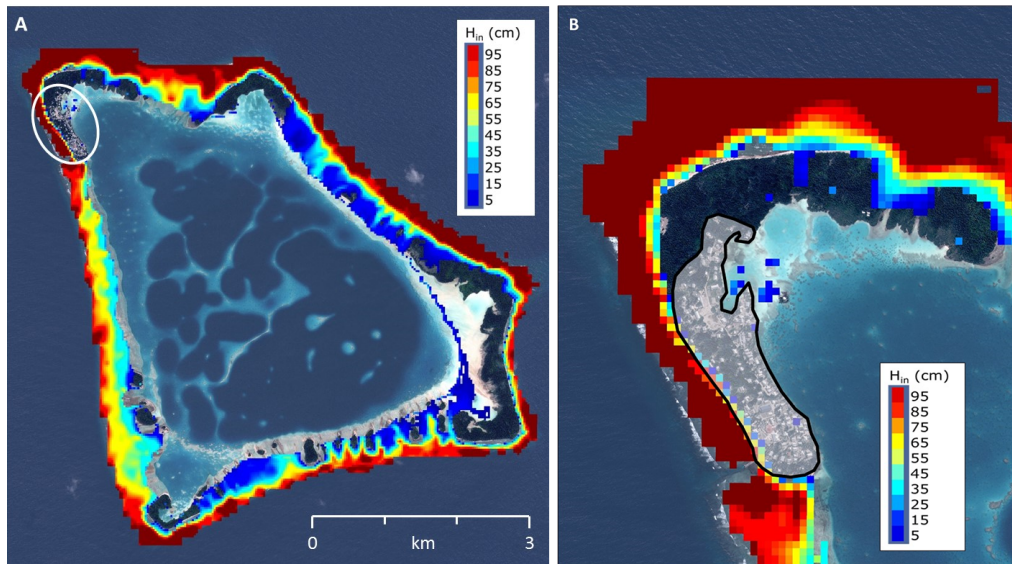


Figure 7. (a) Modelled maximum inundation for the atoll Atafu using the maximum estimates from all distant-earthquake source simulations. (b) Zoomed-in image of the modelled tsunami-flood inundation depths (v) for the village on Atafu in the northwestern corner of the atoll (indicated by the semi-transparent grey area) from all distant-earthquake sources. For both images, the colour bar legend shows the maximum tsunami-flood inundation depth (in centimetres a.m.s.l.) above land, H_{in} . The uncoloured areas, where the underlying satellite image of the atoll and islets can be seen, are emergent land areas that remain dry during the modelled tsunami flooding events. The area of the village is circled in white (a) and outlined by the semi-transparent grey area (b). The lagoon and fringing reef are not considered land and are low-lying so have no colour, but because these areas are so shallow on occasion one or two grid squares of colour might occur away from the known areas of land.

Tokelau tsunami hazard potential

A. R. Orpin et al.

Title Page

Abstract

Introduction

Conclusions

References

Tables

Figures

◀

▶

◀

▶

Back

Close

Full Screen / Esc

Printer-friendly Version

Interactive Discussion

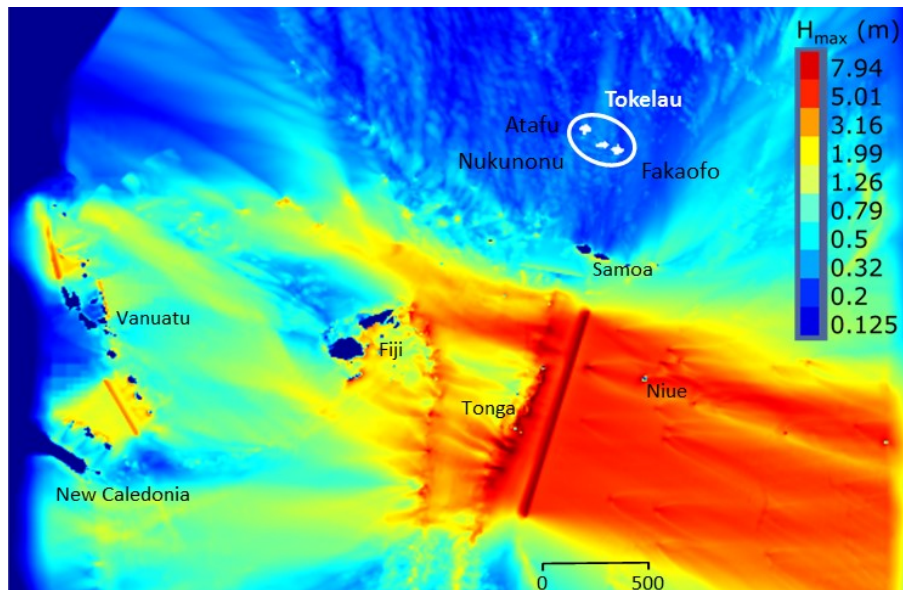


Figure 8. Maximum wave heights (a.m.s.l.) for the compilation of maximum-regional source simulations (the colour scale for H_{\max} shows 0.125 m in dark blue to 7+ m in red). The atolls of Tokelau is indicated in white and circled (upper right).

Tokelau tsunami hazard potential

A. R. Orpin et al.

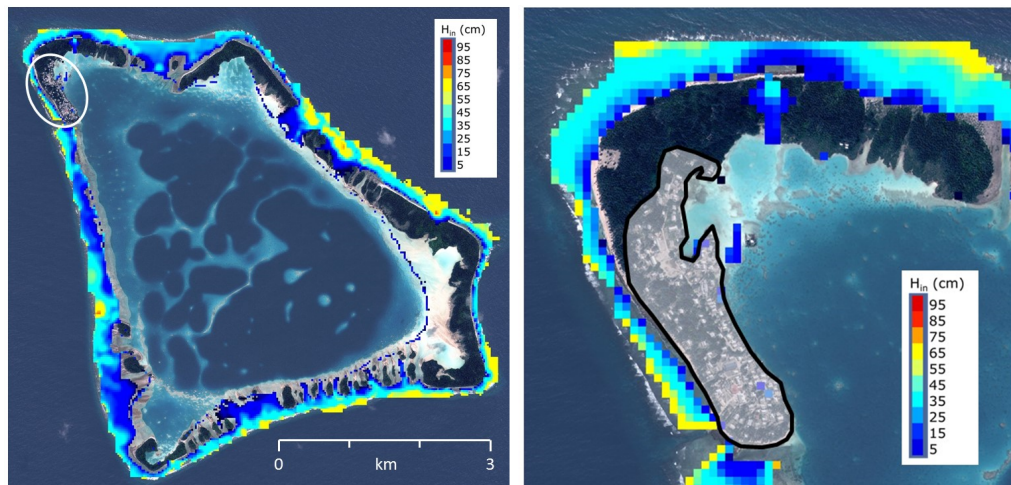
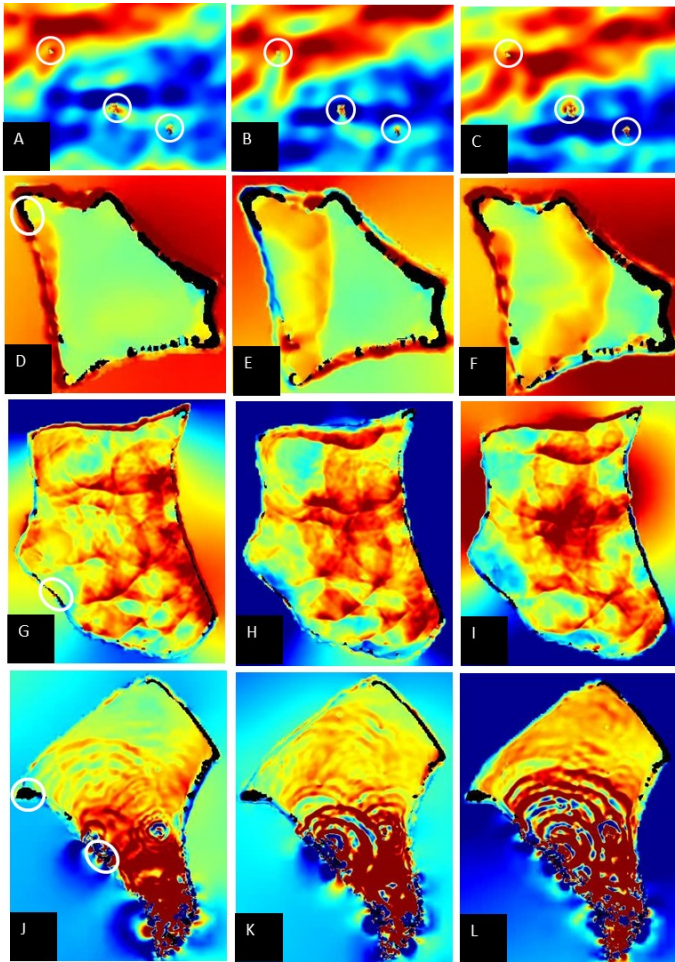


Figure 9. (a) Modelled tsunami-flood inundation depths (a.m.s.l.) on the atoll of Atafu from all regional-earthquake sources. The location of the village is outlined by the white ellipse. (b) Zoomed-in image of the modelled tsunami-flood inundation depths (a.m.s.l.) for the village on Atafu from all regional-earthquake sources. The land area of the village is indicated by the semi-transparent grey area.

[Title Page](#)[Abstract](#)[Introduction](#)[Conclusions](#)[References](#)[Tables](#)[Figures](#)[⏪](#)[⏩](#)[⏴](#)[⏵](#)[Back](#)[Close](#)[Full Screen / Esc](#)[Printer-friendly Version](#)[Interactive Discussion](#)



0.6 0.7 0.8 0.9 1.0 1.1 1.2 1.3 1.4

4432

NHESSD

3, 4391–4433, 2015

Tokelau tsunami hazard potential

A. R. Orpin et al.

[Title Page](#)

[Abstract](#)

[Introduction](#)

[Conclusions](#)

[References](#)

[Tables](#)

[Figures](#)

[I◀](#)

[▶I](#)

[◀](#)

[▶](#)

[Back](#)

[Close](#)

[Full Screen / Esc](#)

[Printer-friendly Version](#)

[Interactive Discussion](#)



Figure 10. Illustrative snapshots of wave fields within atolls generated from the Kuril-source MHWS simulation. Columns show water heights (relative to initial value at MHWS) for successive 100 s increments progressing from left to right in all three columns, the left-hand column at 1 h after the first wave-train arrival at Atafu. The top row (**a–c**) shows the oceanic wave field, the location of the three atolls within the white circles (Atafu, Nukunonu, and Fakaofu from left to right). The second row of frames (**d–f**) focuses on Atafu and follows the same time-sequence as the top row, and similarly for Nukunonu (**g–i**), and Fakaofu (**j–l**). The colour scale bar along the base of the columns indicates the range of water heights from 0.5 to 1.5 m above MHWS.

Tokelau tsunami hazard potential

A. R. Orpin et al.

[Title Page](#)[Abstract](#)[Introduction](#)[Conclusions](#)[References](#)[Tables](#)[Figures](#)[|◀](#)[▶|](#)[◀](#)[▶](#)[Back](#)[Close](#)[Full Screen / Esc](#)[Printer-friendly Version](#)[Interactive Discussion](#)